# Long-term Correlations and $1/f^\alpha$ Noise in the Steady States of Multi-Species Resistor Networks

C. Pennetta, E. Alfinito, and L. Reggiani
*Dipartimento di Ingegneria dell'Innovazione, Università del Salento and Consorzio Nazionale Interun. per le Scienze Fisiche della Materia (CNISM), Via Arnesano, I-73100, Lecce, Italy.**
(Dated: February 6, 2008)

We introduce a multi-species network model which describes the resistance fluctuations of a resistor in a non-equilibrium stationary state. More precisely, a thin resistor characterized by a $1/f^\alpha$ resistance noise is described as a two-dimensional network made by different species of elementary resistors. The resistor species are distinguished by their resistances and by their energies associated with thermally activated processes of breaking and recovery. Depending on the external conditions, stationary states of the network can arise as a result of the competition between these processes. The properties of the network are studied as a function of the temperature by Monte Carlo simulations carried out in the temperature range $300 \div 800$ K. At low temperatures, the resistance fluctuations display long-term correlations expressed by a power-law behavior of the auto-correlation function and by a value $\approx 1$ of the $\alpha$-exponent of the spectral density. On the contrary, at high temperatures the resistance fluctuations exhibit a finite and progressively smaller correlation time associated with a non-exponential decay of correlations and with a value of the $\alpha$-exponent smaller than one. This temperature dependence of the $\alpha$ coefficient reproduces qualitatively well the experimental findings.

PACS numbers: 05.40.-a, 72.70.+m, 61.43.-j, 64.60.Ak
Keywords: Resistor networks, fluctuation phenomena, 1/f noise, disordered materials

## I. INTRODUCTION

Since a long time the analysis of the resistance fluctuations has turned out to be a very powerful tool for probing various condensed matter systems [1, 2] and, in particular, disordered materials [1, 2, 3, 4, 5] like conductor-insulator composites [6], granular systems [7], porous [8] or amorphous materials [9, 10, 11] and organic conducting blends [12]. Therefore, many experimental and theoretical investigations have been devoted to study the properties of the resistance noise as a function of temperature, bias strength and of the main material parameters [1, 2, 6, 7, 8, 9, 10, 11, 12, 13, 14, 15, 16, 17]. Only few studies have considered the behavior of disordered materials over the full range of bias values, by analyzing under a unified approach the linear regime and the nonlinear regime up to the threshold for electrical breakdown [6, 18, 19, 20], even though this kind of studies can provide significant insights about basic properties of the response of nonequilibrium systems [6, 17, 18, 19, 20, 21, 22, 23].

In previous works we have introduced [24] and developed the Stationary and Biased Resistor Network (SBRN) model [19, 20, 25, 26] which is based on a resistor network approach [3, 4, 5] and which allows the study of the electrical conduction and noise of disordered materials over the full range of bias values. This model describes a disordered conducting material as a resistor network whose structure is determined by a stochastic competition between a biased percolation [27, 28] of "broken" resistors (high resistivity resistors) and a biased recovery process (which restores the "regular" resistors with "normal" resistivity) [19, 24]. The SBRN model provides a good description of many features associated with the resistance fluctuations in nonequilibrium stationary states of disordered resistors [6, 12, 19, 20, 25, 29], with resistor trimming processes [30] and with agglomeration and thermal instability phenomena in metallic films [31, 32]. Further successful applications of the model concern the study of electrical breakdown phenomena in composite and granular materials [6, 19, 20, 25], including electromigration damage of metallic lines [16, 26, 33].

However, this model only applies to systems characterized by a Lorentzian noise [1], i.e. by a power spectral density of the resistance fluctuations scaling as $1/f^2$ at high frequencies and becoming flat at frequencies below the so called corner value $f_c$. The existence of a corner frequency in the spectrum corresponds in the time domain to the existence of a well defined characteristic time, $\tau$ (correlation time), associated with the decay of the correlations in the resistance fluctuations [1]. In the particular case of Lorentzian noise this decay is exponential, i.e. the auto-correlation function of the resistance fluctuations is given by [1]:

$$C_{\delta R}(t) \equiv \langle \delta R(t) \delta R(t+\tau) \rangle = \langle (\Delta R)^2 \rangle \exp(-t/\tau) \quad (1)$$

where $\langle (\Delta R)^2 \rangle$ is the variance of the resistance fluctuations. On the other hand, it is well known [1] that at low frequencies many condensed matter systems display $1/f$ resistance noise, i.e. a spectral density scaling over several frequency decades as $1/f^\alpha$, with $\alpha \approx 1$. The amazing presence of $1/f$ noise in a large variety of natural phenomena represents a puzzling problem not yet fully solved. Therefore, a huge quantity of models providing signals with $1/f$ noise have been proposed

*Electronic address: cecilia.pennetta@unile.it

[1, 2, 7, 9, 34, 35, 36, 37, 38, 39, 40, 41, 42, 43]. In particular, the ubiquity of the $1/f$ noise has given rise to many attempts to explain it in terms of a universal law. One simple way to obtain a $1/f$ spectrum is by superimposing a large number of Lorentzian spectra with an appropriate distribution of the correlation times: $D(\tau) \propto 1/\tau$, distributed over many orders of magnitude of $\tau$ values [1]. In some cases, the distribution of the correlation times of the elementary processes contributing to the $1/f$ spectrum can be derived from the distribution of some variable on which the correlation times themselves depend, as in the case of the pioneering works of Mc Whorter [1] and Dutta and Horn [1]. In particular, these authors proposed [1] that the origin of the $1/f$ noise can be attributed to a thermally activated expression of the correlation times, associated with a broad distribution of the corresponding activation energies, an assumption physically plausible for many systems. On the other hand, many other important contributions to the understanding of the $1/f$ noise have been advanced in the last twenty years, which have shown that the presence of a $1/f$ spectrum can also arise from other basic reasons [2, 7, 9, 34, 35, 36, 37, 38, 39, 40, 41, 42, 43]. The dynamical random network model [34] and other spin-glasses models [1, 34] provide a good explanation of the $1/f$ noise in conducting random magnetic materials. Dissipative self-organised criticality (SOC) models, started from the famous work of Bak, Tang and Wiesenfeld [35], clarify the origin of $1/f$ spectra in certain dissipative dynamical systems naturally evolving into a critical state. Avalanche models [36], clustering models [37] and percolative models [7, 9, 38, 39, 40] represent other relevant classes of theoretical approaches explaining the appearence of $1/f$ noise in a variety of systems. Thus, the conclusion, now largely accepted in the literature [1, 2, 40], is that a unique, universal origin of $1/f$ does not exist, even though classes of systems can share a common basic origin of $1/f$ noise.

The aim of this paper is to present a new model which includes and extends to systems characterized by $1/f^{\alpha}$ noise the main feature of the SBRN model, i.e. the stochastic competition between thermally activated and biased processes of breaking and recovery of the elementary resistors of a network [19]. Actually, this feature has turned out to be essential for the success of the SBRN model in the description of the wide phenomelogy associated with the resistance fluctuations of disordered resistors, in both nonequilibrium stationary states and nonstationary failure states [6, 12, 26, 29, 30, 31, 32]. To this purpose, here we study a network made by several species of resistors, where each species is characterized by a resistance value and by a pair of activation energies associated with the breaking and the recovery processes. For this reason we call this model "multi-species network" (MSN) model. The states, either stationary or nonstationary, of the MSN result from the stochastic competition between these processes of breaking and recovery involving the elementary resistors. In analogy with the Dutta and Horn model [1], we take the breaking and recovery activation energies distributed in a broad range of values. A choice physically justified in disordered systems, like granular and amorphous materials, composites, etc. where the orientational disorder present inside these materials can give rise to different energy barriers for the electron flow along the different conducting paths [1, 3, 4, 34]. As a result, the resistance fluctuations of the MSN exhibit a $1/f^{\alpha}$ spectrum, where the value of $\alpha$ depends on the external conditions (temperature and electrical bias). In particular, in this paper, we discuss the states of a MSN as a function of the temperature and in the linear regime of the external bias, when Joule heating effects are negligible.

The paper is organised as follows: in Sect. II we illustrate the MSN model, while in Sect. III we report the results by focusing in particular on the role played by the temperature on the fluctuations properties of the multi-species network. Finally, in Sect. IV we draw the conclusions of this study.

## II. MODEL

According to the SBRN model [19, 20] a conducting thin film with granular structure is described as a two-dimensional square-lattice resistor network [3, 5]. For simplicity here we study a network $N \times N$ (where $N$ is the linear size of the network), even if networks with a different geometry can be considered [26]. The network is biased by an external constant current, $I$, applied through perfectly conducting bars placed at the left and right hand sides and it lies on an insulating substrate at a given temperature $T$, which acts as a thermal bath. Each resistor can be in two different states: i) regular, corresponding to a resistance $r_n = r_0[1 + \alpha_T(T_n - T)]$, where $\alpha_T$ is the temperature coefficient of the resistance and $T_n$ is the local temperature and ii) broken, corresponding to an effectively "infinite" resistance, $r_{OP} = 10^9 r_n$. Resistors in the broken state will be called defects. The temperature $T_n$ is expressed as [28]:

$$T_n = T + A[r_n i_n^2 + \frac{D}{N_{neig}} \sum_l (r_l i_l^2 - r_n i_n^2)] \qquad (2)$$

where $D = 3/4$, the sum is performed over the $N_{neig}$ nearest neighbors of the n-*th* resistor and $i_n$ is the current flowing in it. The above expression of $T_n$ takes into account the Joule heating of the n-*th* resistor [27, 28, 44] and the thermal exchanges with its neighbors [28]. The importance of both these effects is controlled by the parameter $A$, thermal resistance, which describes the heat coupling of each resistor with the substrate [19, 27, 44]. We note that by adopting Eq.(2) we are assuming for simplicity an instantaneous thermalization of each resistor and we are neglecting time dependent effects discussed in Ref. [44].

In the initial state of the network all the resistors are taken to be identical: $r_n \equiv r_0$. The SBRM model then

assumes that the evolution of the network is determined by the competition between two biased stochastic processes: one of breaking and the other of recovery. The former process consists in the transition of an elementary resistor from the regular to the broken state and it occurs with a thermally activated probability [27]:

$$W_{Dn} = \exp(-E_D/k_B T_n) \tag{3}$$

the latter process consists in the reverse transition and it occurs with probability [19, 24]:

$$W_{Rn} = \exp(-E_R/k_B T_n) \tag{4}$$

where $E_D$ and $E_R$ are the activation energies of the two processes and $k_B$ the Boltzmann constant. The time evolution of the network is then obtained by Monte Carlo simulations which update the network resistance after a sweep of breaking and recovery processes, according to an iterative procedure detailed in Ref. [19]. The sequence of successive network configurations provides a resistance signal, $R(t)$, after an appropriate calibration of the time scale. Then, depending on the stress conditions ($I$ and $T$) and on the network parameters (size, activation energies, $r_0$, $\alpha_T$ and $A$), the network either reaches a steady state or undergoes an irreversible electrical failure [19, 20, 25, 26]. This latter possibility is associated with the achievement of the percolation threshold, $p_c$, for the fraction of broken resistors [5]. Therefore, for a given network at a given temperature, a threshold current value, $I_B$, exists above which electrical breakdown occurs [19]. For values of the applied current below this threshold, the steady state of the network is characterized by fluctuations of the fraction of broken resistors, $\delta p$, and of the resistance, $\delta R$, around their respective average values $\langle p \rangle$ and $\langle R \rangle$.

The network described above, as provided by the SBRN model, is made by a single species of resistors, all characterized by the same values of $r_0$, $\alpha_T$, $E_D$ and $E_R$. Thus, we can speak of a "single-species network". The disorder inside this network only arises from the fact that some resistors can be in the broken state. As a consequence, current and temperature are not homogeneously distributed [26, 27], thus implying inhomogeneous probabilities of breaking and recovery and, through the temperature coefficient $\alpha_T$, different resistance values of the regular resistors. Furthermore, by analogy with generation-recombination noise in a two-levels system, this model describes a system characterized by a single time scale and thus by Lorentzian noise. To overcome the above limitations here we consider a network made by $N_{spec}$ species of resistors, i.e. a "multi-species network" (MSN). Each species is characterized by different values of the parameters: $r_{0,i}$, $\alpha_{T,i}$, $E_{D,i}$ and $E_{R,i}$ with $i = 1, ...N_{spec}$. Then, an "identity" (an index $i$) is attributed at random to each resistor. In the initial state of the network the species are taken to be present with the same number of resistors. As a reasonable choice, we have taken $r_{0,i}$ uniformly distributed inside a given range of resistance values: $r_{0,i} \in [r_{min}, r_{max}]$, while other options are as well reasonable. We limit the present study to the linear regime in the external bias, when Joule heating effects are negligible, i.e. $T_n \equiv T$, $\forall n$ and consequently $r_{n,i} \equiv r_{0,i}$, $\forall n$ and $\forall i$. Alternatively, we can say that we study a system characterized by negligibly small values of the thermal resistance and of the resistance temperature coefficients: $A = 0$ and $\alpha_{T,i} = 0$, $\forall i$. We stress that the linear regime condition corresponds to uniform probabilities of breaking and recovery for the resistors belonging to each given species [28, 45]. Therefore, the results that we will report in Sect. III directly generalize the results of Ref. [45] to systems characterized by $1/f^\alpha$ resistance noise. The limitation to the linear regime of currents has been adopted here for simplicity and also because we aim to focus on the temperature dependence of the correlation properties of the resistance fluctuations. However, we underline that there is no special difficulty in extending this study to the nonlinear regime in the applied bias. In this respect, it must be noted that we expect that all the other significant features associated with the SBRN model (existence of a threshold current for breakdown [19, 20], dependence of $\langle R \rangle$ and $\langle (\Delta R)^2 \rangle$ on the bias [19], times to failure distribution [26], non-Gaussianity of the resistance fluctuations [20, 25], role of the network geometry [26], etc.) remain unchanged for a MSN network.

The values of the activation energies $E_{D,i}$ and $E_{R,i}$ for the different resistor species have been chosen as follows. In Ref. [45] it was proved that for a single-species network, when the average fraction of defects $\langle p \rangle$ is sufficiently far from the percolation threshold ($p_c = 0.5$ for a $N \times N$ square-lattice network [5]), the correlation time of the resistance fluctuations is approximated by:

$$\frac{1}{\tau} = W_D + \frac{W_R}{(1 - W_R)} = \frac{W_D}{\langle p \rangle} \tag{5}$$

where $W_D$ and $W_R$ are the thermal activated probabilities defined by the Eqs. (3)-(4) and calculated for $T_n = T$. In other terms, Eq. (5) implies that at a given temperature, both $\langle p \rangle$ and $\tau$ only depend on $E_D$ and $E_R$. This equation can thus be inverted to determine $E_D$ and $E_R$ as functions of $\langle p \rangle$ and $\tau$. These considerations can be generalized to the case of a multi-species network by giving the criterion for a convenient choice of the activation energies. To this purpose, first we choose a reference value of the substrate temperature, $T_{ref}$, and a set of values of the average defect fraction, $\langle p_i \rangle$, corresponding to the different resistor species (where $p_i \equiv N_{brok,i}/N_{tot,i}$ with $i = 1, ..., N_{spec}$). Second, by considering the correlation times, $\tau_i$, associated with the fluctuations [46] of $p_i$, we choose the values of the activation energies $E_{D,i}$ and $E_{R,i}$ in such a way to obtain a logarithmic distribution of $\tau_i$ inside a sufficiently wide interval: $\tau_i \in [\tau_{min}, \tau_{max}]$. The different $\tau_i$ are then attributed to the different resistor species by adopting the criterion that increasing values of $\tau_i$ are paired with increasing values of $r_{0,i}$. Alternative choices are of course possible.

All the results reported here are obtained by applying a bias current $I = 1.0$ (A) to a network of sizes $75 \times 75$ made by $N_{spec} = 15$ resistor species and by choosing $r_{min} = 0.5$ $\Omega$ and $r_{max} = 1.5$ $\Omega$. Furthermore we take: $T_{ref} = 300$ K, $\langle p_i \rangle \approx 0.25 \ \ \forall i$, $\tau_{min} \approx 2$ and $\tau_{max} \approx 5 \times 10^5$ (where times are expressed in units of iterative steps). We underline that the choice made above for the values of $T_{ref}$, $\langle p_i \rangle$, $\tau_{min}$ and $\tau_{max}$, determines once for all (i.e. for all the temperatures) the set of activation energies $E_{D,i}$ and $E_{R,i}$. In the present case $E_{D,i}$ and $E_{R,i}$ are in the range $58 \div 375$ meV and $37 \div 346$ meV, respectively. In fact, the values of $E_{D,i}$ and $E_{R,i}$, together with $r_{0,i}$ and $N_{spec}$, determine the intrinsic properties of the material under test. Therefore, when performing a simulation at temperatures different from $T_{ref}$, the values of $\tau_i$ recalculated from Eq. (5) are the input parameters of the simulation, while the values of $\langle p_i \rangle$ only serve as a check of consistency with those obtained directly from the output of the simulation. As a general trend, by increasing the temperature the range of values of $\tau_i$ becomes more narrow and the values of $\langle p_i \rangle$ increase progressively.

The time evolution of the network is then obtained by Monte Carlo simulations according to the iterative procedure described in details in Ref. [19]. The auto-correlation functions and the power spectral densities of the resistance fluctuations are calculated by analyzing stationary signals $R(t)$ consisting of $2 \times 10^6$ records.

## III. RESULTS

The resistance evolution of a multi-species network calculated at a temperature of 300 K is reported in Fig. 1. The inset displays a small part of the same evolution over an enlarged time scale. The co-existence of different characteristic time scales in the $R(t)$ signal is clearly shown in Fig. 1, where the long relaxation time associated with the achievement of the steady state, $\tau_{rel}$, co-exists with the shorter times characterizing the resistance fluctuations displayed in the inset. For comparison, we report in Fig. 2 the time evolution of the resistance of a single-species network obtained at $T = 300$ K by the SBRN model. In this case, the values of the activation energies ($E_D = 350$ meV and $E_R = 310$ meV) are chosen to give a relaxation time comparable with that of the signal in Fig. 1. The behavior of the resistance is now determined by a single time scale ($\tau \approx \tau_{rel}$) and thus it is less noisy and essentially flat over time scales shorter than $\tau$. This is emphasized by the inset of Fig. 2 where the stochastic signal resembles that of a few level system (it must be noted that the vertical scale of the inset in Fig. 2 is significantly enhanced with respect to that of Fig. 1).

Figure 3 reports the auto-correlation functions of the resistance fluctuations on a log-log plot. More precisely, the auto-correlation function corresponding to the multi-species network (MSN model) is shown by black triangles while that corresponding to the single-species network (SBRN model) is reported by black squares. The

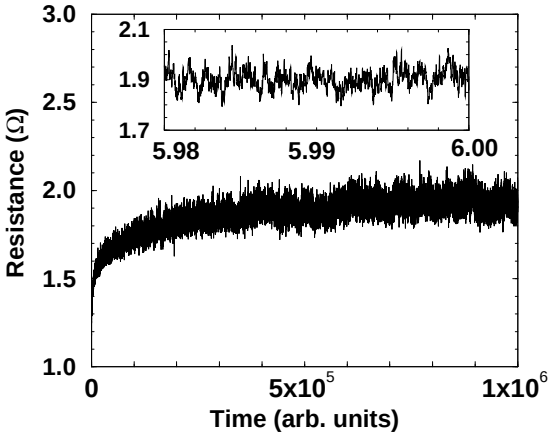


FIG. 1: Resistance evolution of a multi-species network (MSN model) calculated at 300 K. The resistance is espressed in Ohm and the time in iterative steps. The inset highlights the resistance fluctuations on an enlarged time scale. In particular, the time units are divided by a factor $10^{-5}$.

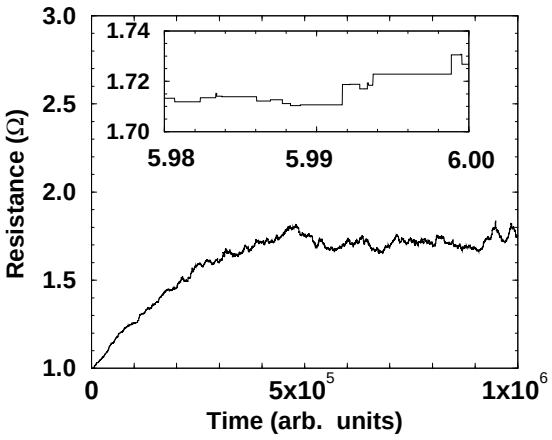


FIG. 2: Resistance evolution of a single-species network (SBRN model) calculated at 300 K. The resistance is espressed in Ohm and the time in iterative steps. The inset displays the resistance fluctuations on the same enlarged time scale of the inset in Fig. 1. (the vertical scales of the insets in the two figures are different).

solid and short dashed lines represent the best-fits to the two $C_{\delta R}$ functions carried out respectively with a power-law and with an exponential law. The fitting procedure confirms the exponential decay of the correlations in the resistance fluctuations of the single-species network, described by Eq. (1), and points out the existence of long-term correlations in the resistance fluctuations of the multi-species-network, characterized by a power-law decay of the auto-correlation function:

$$C_{\delta R}(t) \sim t^{-\gamma} \tag{6}$$

with $0 < \gamma < 1$. In particular, for the case of Fig. 3 we have found a value $\gamma = 0.22$ for the correlation exponent. We stress that the above expression of the

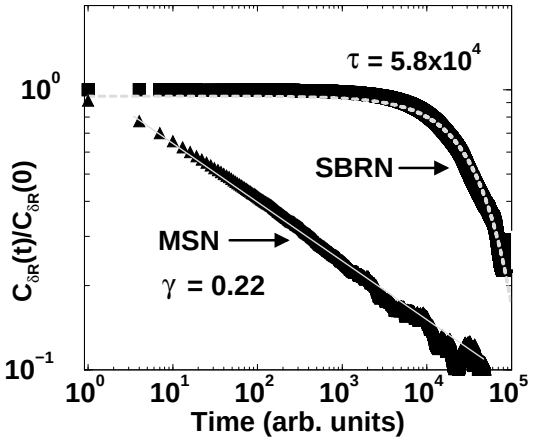


FIG. 3: Auto-correlation functions of the resistance fluctuations calculated for a multi-species network (MSN model, black triangles) and for a single-species network (SBRN model, black squares). Both functions are obtained at 300 K. The solid and short dashed grey lines show the best-fit respectively with a power-law of exponent $\gamma = 0.22$ and with an exponential function with correlation time $\tau = 5.8 \times 10^4$. The time is expressed in iterative steps.

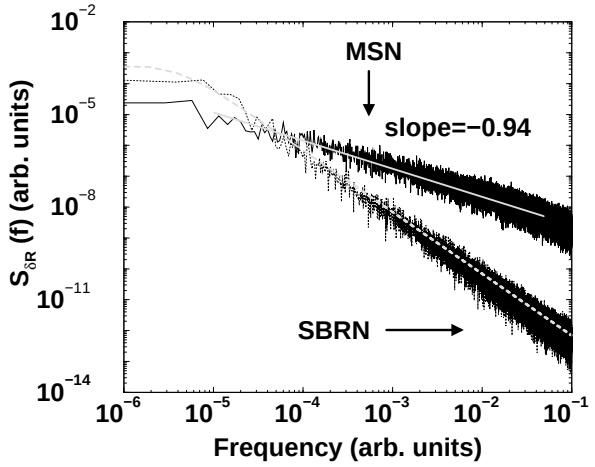


FIG. 4: Power spectral density of the resistance fluctuations at 300 K calculated for the multi-species network (MSN model, solid line) and for the single-species network (SBRN model, dotted line). The grey solid line shows the best-fit to the MSN spectrum with a power-law of slope -0.94. The grey dashed curve represents the best-fit with a Lorentzian to the SBRN spectrum.

auto-correlation function implies a divergence of the correlation time, as can be easily seen by considering the following general expression of the correlation time [47]:

$$\tau = \int_0^\infty \frac{C_{\delta R}(t)}{C_{\delta R}(0)} dt \qquad (7)$$

The power spectral densities of the resistance fluctuations calculated at 300 K by the MSN model and by the SBRN model are displayed in Fig. 4. The grey solid line represents the best-fit with a power-law to the MSN spectrum. The grey dashed curve is the best-fit with a Lorentzian to the SBRN spectrum. The corner frequency of the Lorentzian, $f_c = 4.0 \times 10^{-6}$ (arbitrary units), is consistent with the correlation time reported in Fig. 3 and obtained by the best-fit of the corresponding auto-correlation function. Thus, Fig. 4 shows that at 300 K the resistance fluctuations of the multi-species network exhibit a power spectral density scaling as $1/f^\alpha$ over several decades of frequency, with a value $\alpha = 0.94$. This result is a consequence of the envelope of the different time scales associated with the different resistor species.

Now, we will analyze the effect of the temperature on the resistance fluctuations of a multi-species network. To this purpose, Fig. 5 displays the resistance evolutions calculated at increasing temperatures: $T = 400$ K (lower curve) and $T = 600$ K (upper curve). Already the qualitative comparison of the $R(t)$ signals in Figs. 1 and 5, shows that at increasing temperature there is a significant growth of both the average resistance and the variance of the resistance fluctuations (we will discuss in detail the behavior of these quantities in the following). Moreover, these figures point out a drastic reduction of the relaxation time at increasing temperature (more than one order of magnitude when $T$ rises from 300 K to 400 K).

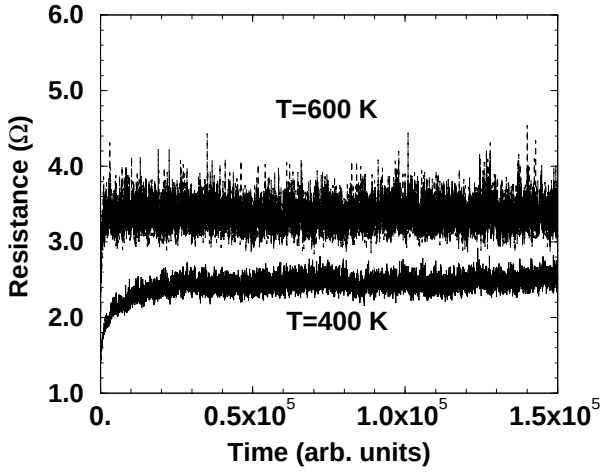


FIG. 5: Resistance evolution of a multi-species network at 400 K and 600 K. The resistance is espressed in Ohm and the time in iterative steps.

The temperature is also found to affect the distribution of the resistance fluctuations by increasing its skewness, as shown in Fig. 6, which reports on a lin-log plot the probability density function (PDF, here denoted by $\phi$), of the distribution of the resistance fluctuations. A normalized representation has been adopted for convenience (here $\sigma$ is the root mean square deviation from the average resistance). In Fig. 6, the different symbols represent the PDFs calculated in the steady state of the multi-species network at 300 K (full diamonds), 400 K (open

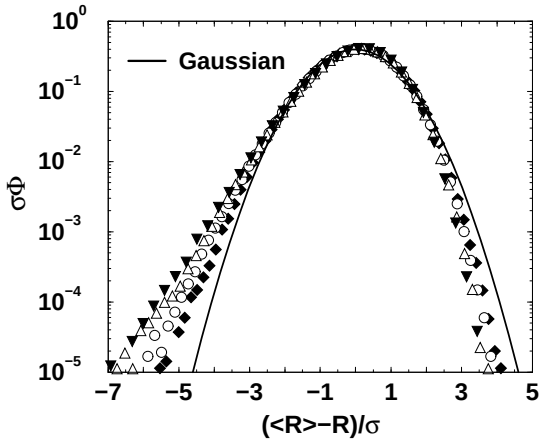


FIG. 6: Normalized probability density functions of the resistance fluctuations of a multi-species network calculated at 300 K (full diamonds), 400 K (open circles), 500 K (open up-triangles) and 600 K (full down-triangles); $\sigma$ is the root-mean-square deviation from the average resistance value. The solid black curve shows the normalized Gaussian distribution.

circles), 500 K (open up-triangles) and 600 K (full down-triangles). For comparison, the normalized Gaussian distribution has been also reported as a solid line. The figure shows a significant non-Gaussianity of the resistance fluctuations, which becomes stronger at high temperatures, meaning that the system is approaching failure conditions. The distribution of the resistance fluctuations and the role played on the non-Gaussianity by the size, shape and disorder of the network has been investigated in Refs. [20, 25], where the link with the universal distribution of fluctuations of Bramwell, Holdsworth and Pinton [48, 49] has been discussed.

Figure 7 reports the auto-correlation functions of the resistance fluctuations of a multi-species network calculated at 400 K and 600 K. For comparison, the $C_{\delta R}$ function obtained at 300 K (already shown in Fig. 3) has been drawn again in Fig. 7 with the solid grey line still giving the best-fit with a power-law. The dashed grey curves instead represent the best-fit to the $C_{\delta R}$ functions at 400 K and 600 K with the expression:

$$C_{\delta R}(t) = C_0 t^{-h} \exp(-t/u) \tag{8}$$

The values of the best-fit parameters are: $C_0 = 1.13$, $h = 0.30$ and $u = 1.42 \times 10^4$ for $T = 400$ K and $C_0' = 0.965$, $h' = 0.46$ and $u' = 5.57 \times 10^2$ for $T = 600$ K. As pointed out by Fig. 7, the fit to $C_{\delta R}$ with Eq. (8) is very satisfying. We thus conclude that at high temperatures the auto-correlation function of the resistance fluctuations of the multi-species network is well described by a power-law with an exponential cut-off. Such kinds of mixed decays of the correlations, non-exponential and non power-law, are often found in the transition of a complex system from short-term correlated to long-term correlated regimes [50, 51]. It should be noted that for $u \to \infty$ Eq. (8) becomes a power-law while for $h \to 0$ it describes an exponential decay.

Actually, Fig. 7 makes evident a strong reduction of the correlation time of the fluctuations when the temperature increases. This result can be easily understood in terms of Eq. (5), by considering the thermally activated expressions of the breaking and recovery probabilities: in fact the increase of temperature implies a significant reduction of the ratio $\tau_{min}/\tau_{max}$. Therefore the interval $[\tau_{min}, \tau_{max}]$ where the $\tau_i$ are distributed becomes more and more narrow, destroying the power-law decay of correlations and giving rise to an exponential tail. It must be noted that, for similar reasons, when the temperature decreases below the reference value, $T < T_{ref}$, the ratio $\tau_{min}/\tau_{max}$ strongly increases and the correlations in the resistance fluctuations keep their power-law decay over wider time scales (for example, when $T = 200$ K the ratio $\tau_{min}/\tau_{max}$ becomes $7.5 \times 10^7$). $T_{ref}$ is thus closely related to the transition temperature, $T^*$, from a long-term correlated behavior i.e. a behavior characterized by a divergent correlation time and occurring for $T < T^*$, to a behavior characterized by a finite correlation time and occurring for $T > T^*$.

The correlation time of the resistance fluctuations can be directly estimated at $T > T_{ref}$ by considering Eq. (7) and making use of Eq. (8). We obtain the following expression of $\tau$ in terms of the best-fit parameters of the auto-correlation function:

$$\tau = u^{1-h}\Gamma(1-h) \tag{9}$$

where $\Gamma$ is the Gamma function. The values of $\tau$ calculated in such a way are reported in Fig. 8 as a function of the temperature. The figure shows a strong increase of $\tau$ at decreasing temperatures, when $T$ approches $T_{ref}$, in fact for this value of temperature $\tau$ is expected to diverge consistently with the power-law behavior of the auto-correlation function. To highlight the dependence of $\tau$ on the temperature, we report in Fig. 9 a log-log plot of the correlation time as a function of the difference $T - T^*$, where the value of the transition temperature $T^* = 306$ K is determined by a best-fit to the data in Fig. 8 with the power-law: $\tau \sim (T - T^*)^{-\theta}$. The fitting curve is displayed in Fig. 9 by the dashed straight line. We find a value $\theta = 2.7$ for the exponent. Therefore Fig. 9 shows that the dependence of the correlation time on temperature is well described by a power of $T - T^*$, where the transition temperature $T^* \approx T_{ref}$.

The power spectral densities of the resistance fluctuations calculated at the temperatures of 400 K and 600 K are reported in Fig. 10. Here the grey lines represent the best-fit with power-laws of slopes -0.87 and -0.78, respectively. Thus we find that the power spectrum keeps the $1/f^\alpha$ form also at high temperatures. However, the value of the exponent $\alpha$ decreases to values well below unity when $T > T^*$. This dependence of $\alpha$ on temperature has been studied since a long time [1, 10]. A qualitative description of this dependence is provided by the well known Dutta-Horn relation [1]. On the other hand,

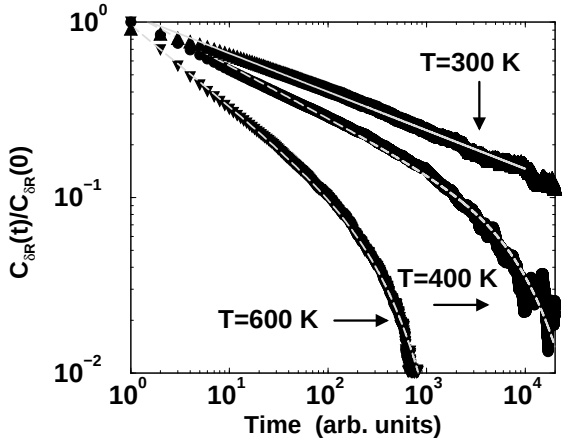


FIG. 7: Auto-correlation functions of the resistance fluctuations of a multi-species network calculated at different temperatures. The solid grey curve shows the best-fit with a power-law to the auto-correlation function at 300 K (the same of Fig. 3). The dashed grey curves display the best-fit to the auto-correlation functions at 400 and 600 K with the function: $C(t) = C_0 t^{-h} \exp[-t/u]$ (see the text for the values of the fit parameters). The time is expressed in iterative steps.

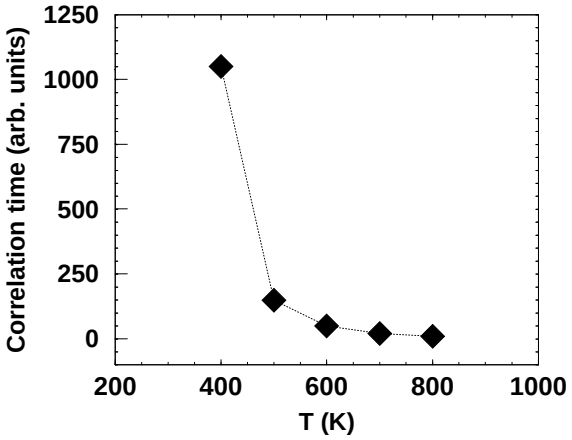


FIG. 8: Correlation time of the resistance fluctuations as a function of the temperature. The time is expressed in iterative steps and the temperature in K. The dotted line connecting the diamonds is a guide to the eyes.

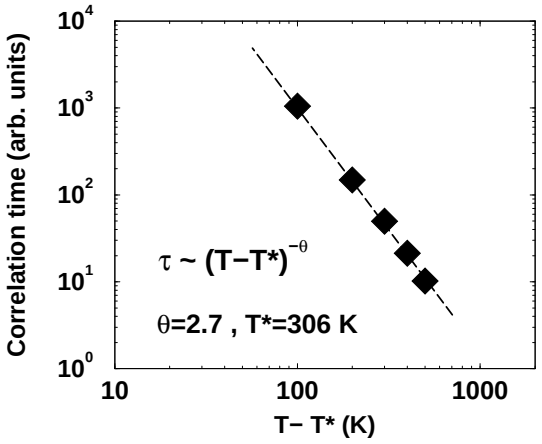


FIG. 9: Correlation time of the resistance fluctuations as a function of the difference $T - T^*$. The time is expressed in iterative steps and the temperature in K. The value of $T^*$ is reported in the figure. The dashed line shows the fit with a power-law of exponent $\theta = 2.7$.

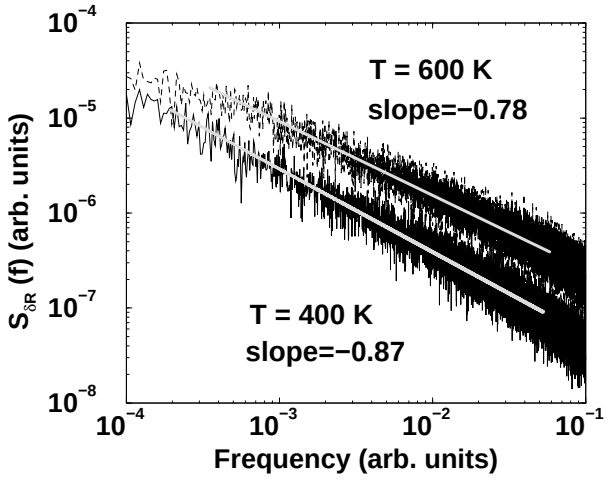


FIG. 10: Power spectral density of the resistance fluctuations of the multi-species network at $T = 400$ K and $T = 600$ K. The grey lines show the best-fit with power-laws of slopes -0.87 and -0.78, respectively.

many experiments have pointed out a strong dependence of the detailed behavior of $\alpha(T)$ on the particular material [1, 2, 10]. In this respect, it should be noted that a decrease of the $\alpha$ exponent from $\alpha \approx 1$ and $\alpha \approx 0.8-0.5$ is frequently observed in the experiments [1, 2, 10] at intermediate temperatures above 100-200 K, similarly to our case where this decrease occurs above $T_{ref} \approx T^* \approx 300$ K. It should be noted, however, that in our model $T_{ref}$ merely plays the role of an input parameter which can be adapted to fit the experiments. Furthermore, we stress that the monotonic decrease of $\alpha$ for $T > T^*$ is obtained here in the linear regime of currents, i.e. neglecting Joule heating effects. Actually, these effects, whose importance also depends on temperature can give rise to a more complicated behavior of $\alpha$ versus temperature.

Now we consider the dependence on temperature of the average resistance and of the variance of the resistance fluctuations. We call $R_0$ the average value of the resistance in the limit $T = 0$. This value represents the resistance of a network free of broken resistors but in any case disordered (due to the presence of different resistor species). Thus $R_0$ not only depends on the network size and on the set of values $\{r_{0,i}\}$ with $i = 1, ...N_{spec}$, but also on the particular random distribution of the $r_{0,i}$ within the network. Figure 11 displays the difference $\langle R \rangle - R_0$ as a function of the temperature. A log-log representation is adopted here for convenience. The

dashed straight line represents the best-fit of the data with the expression: $\langle R\rangle = R_0 + AT^{\gamma}$, with $\gamma = 0.83$, $A = 1.35 \times 10^{-2}\ \Omega/K^{\gamma}$ and $R_0 = 0.52\ \Omega$. We can see that this expression describes rather well the behavior of the average resistance.

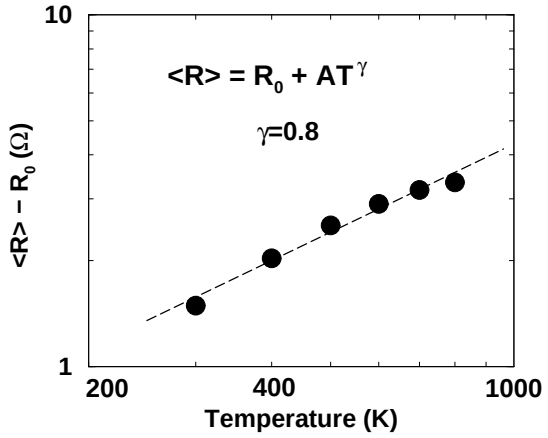


FIG. 11: Variation of the average resistance as a function of the temperature. The resistance is espressed in Ohm and the temperature in K. The dashed straight line represents the best-fit with the expression reported in the figure.

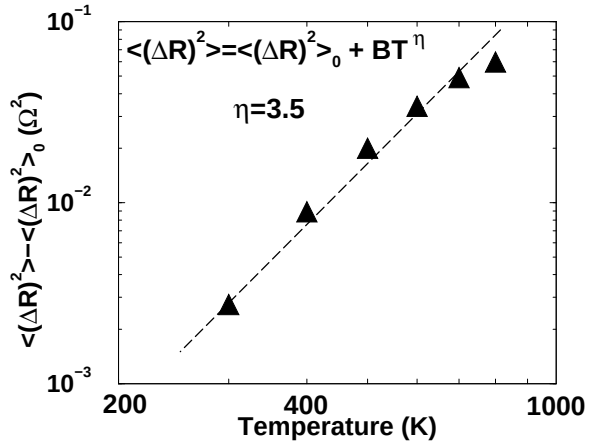


FIG. 12: Change of the variance of the resistance fluctuations as a function of the temperature. The variance is espressed in $\Omega^2$ and the temperature in K. The dashed straight line shows a best-fit with the expression reported in the figure.

The change with the temperature of the variance of the resistance fluctuations is reported in Fig. 12. Here $\langle(\Delta R)^2\rangle_0$ is the limit value of the variance at $T = 0$. This value mainly depends on the network size [45] and it vanishes for $N \to \infty$. Again, a log-log representation is used in this figure. The dashed straight line displays the best-fit with the expression: $\langle(\Delta R)^2\rangle = \langle(\Delta R)^2\rangle_0 + BT^{\eta}$ which is found to provide a good description of the data for $\eta = 3.5$, $B = 7.32 \times 10^{-12}\ \Omega^2/K^{\eta}$ and $\langle(\Delta R)^2\rangle_0 = 5.0 \times 10^{-7}\ \Omega^2$ .

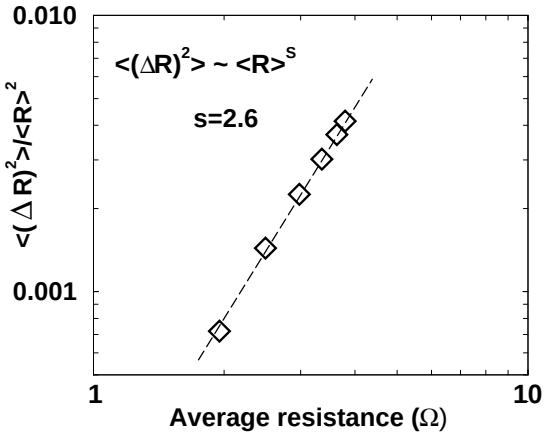


FIG. 13: Relative variance of the resistance fluctuations as a function of the average resistance (this last is expressed in Ohm). The dashed line shows a best-fit with a power-law of exponent $s = 2.6$.

Finally, Fig. 13 shows in a log-log plot the relative variance of the resistance fluctuations as a function of the average resistance. In this case the dashed line represents the best-fit with a power-law of exponent 2.6. In other terms, Fig. 13 shows that:

$$\langle(\Delta R)^2\rangle/\langle R\rangle^2 \ \sim \langle R\rangle^s \qquad (10)$$

where $s = 2.6$. To be consistent with the behaviors of the average resistance and of the variance of the resistance fluctuations reported in Figs. 11-12, the following scaling relation should hold within the exponents $s$, $\eta$ and $\gamma$: $s = \eta/\gamma - 2$. By using the previously reported values of $\eta$ and $\gamma$ we obtain for $s$ the value 2.4, in agreement (within the error) with the result $s = 2.6$ obtained by directly considering the dependence of $\langle(\Delta R)^2\rangle/\langle R\rangle^2$ on $\langle R\rangle$. We underline that both, the behavior of the relative variance and the value of $s$, are perfectly consistent with the results reported in Ref. [45]. This agreement confirms and points out the fact that the model discussed here directly generalizes the results of Ref. [45] to resistors characterized by $1/f^{\alpha}$ resistance noise.

## IV. CONCLUSIONS

We have developed a stochastic model to investigate the $1/f^{\alpha}$ resistance noise in disordered materials. More precisely, we have considered the resistance fluctuations of a thin resistor with granular structure in a non-equilibrium stationary state. This system has been modeled as a two-dimensional network made by different species of elementary resistors. The steady state of this multi-species network is determined by the competition among different thermally activated and stochastic processes of breaking and recovery of the elementary resistors. The network properties have then been studied by Monte Carlo simulations as a function of the temperature and in the linear regime of the external bias. By a suitable choice of the values of the parameters, the

model gives rise to resistance fluctuations with different power spectra, thus providing a unified approach to the study of materials exhibiting either Lorentzian noise or $1/f^{\alpha}$ noise. In particular, by increasing the temperature in the range from 300 to 800 K the $\alpha$ exponent decreases from values near to 1 down to values around 0.5, in qualitative agreement with experimental findings available from the literature [1, 2, 10]. This behavior, indicative of a drastic reduction of the correlation time of the resistance fluctuations, has been also analysed in terms of the auto-correlation functions. These last progressively change at increasing temperature, going from a slow, power-law decay of the correlations at 300 K to a faster but non-exponential decay at higher temperatures.

## ACKNOWLEDGMENTS

Support from MIUR cofin-05 project "Strumentazione elettronica integrata per lo studio di variazioni conformazionali di proteine tramite misure elettriche" is acknowledged.


[1] M. B. Weissman, *Rev. Mod. Phys.*, **60**, 537, (1988); F. N. Hooge, *Rep. Prog. Phys.*, **44**, 479 (1981); P. Dutta and P. M. Horn, *Rev. Mod. Phys.*, **53**, 497 (1981).

[2] *Unsolved Problems of Noise and Fluctuations*, ed. by L. Reggiani, C. Pennetta, V. Akimov, E. Alfinito and M. Rosini, AIP Conf. Proc. **800**, New York (2005); *Noise and Fluctuations*, ed. by T. González, J. Mateos and D. Pardo, AIP Conf. Proc. **780**, New York (2005).

[3] S. Torquato, *Random Heterogeneous Materials, Microscopic and Macroscopic Properties*, Springer-Verlag, New York, 2002.

[4] M. Sahimi, *Phys. Rep.* **306**, 213 (1998).

[5] D. Stauffer and A. Aharony, *Introduction to Percolation Theory*, Taylor & Francis, London (1992).

[6] C. D. Mukherjee and K. K. Bardhan, *Phys. Rev. Lett.* **91**, 025702 (2003); C. D. Mukherjee, K. K. Bardhan and M. B. Heaney, *Phys. Rev. Lett.* **83**, 1215 (1999); U. N. Nandi, C. D. Mukherjee and K. K. Bardhan, *Phys. Rev.* B, **54**, 12903 (1996).

[7] K. M. Abkemeier and D. G. Grier, *Phys. Rev.* B, **54**, 2723 (1996).

[8] I. Bloom and I. Balberg, *Appl. Phys. Lett.*, **74**, 1427 (1999).

[9] L. M. Lust and J. Kakalios, *Phys. Rev. Lett.*, **75**, 2192 (1995); C. Parman and J. Kakalios, *Phys. Rev. Lett.*, **67**, 2529 (1991).

[10] G. B. Alers, M. B. Weissman, R. S. Averback and H. Shyu, *Phys. Rev.* B, **40**, 900 (1989).

[11] G. Snyder, M. B. Weissman, H. T. Hardner and C. Parman, *Phys. Rev.* B, **56**, 9205 (1997).

[12] J. Planes and A. Francois, *Phys. Rev.* B, **70**, 184203 (2004).

[13] K. M. Chen, G. W. Huang, D. Y. Chiu, H. J. Huang and C. Y. Chang, *Appl. Phys. Lett.*, **81**, 2578 (2002).

[14] S. Kar, A. K. Raychaudhuri, A. Ghosh, H. V. Löhneysen and G. Weiss, *Phys. Rev. Lett.*, **91**, 216603 (2003).

[15] C. Chiteme, D. S. McLachlan and I. Balberg, *Phys. Rev.* B, **67**, 024207 (2003).

[16] V. Emelianov, G. Ganesan, A. Puzic, S. Schulz, M. Eizenberg, H. U. Habermeier and H. Stoll, in *Noise as a Tool for Studying Materials*, p. 271, ed. by M. B. Weissman, N. E. Israeloff and A. S. Kogan, Procs. SPIE, **5112**, Int. Soc. Opt. Eng., Bellingham (2004).

[17] N. Garnier and S. Ciliberto, *Phys. Rev.* E, **71**, 060101 (2005).

[18] J. V. Andersen, D. Sornette and K.T. Leung, *Phys. Rev. Lett.* **78**, 2140 (1997); L. Lamaignère, F. Carmona and D. Sornette, *Phys. Rev. Lett.* **77**, 2738 (1996).

[19] C. Pennetta, L. Reggiani, G. Trefán and E. Alfinito, *Phys. Rev.* E, **65**, 066119 (2002); C. Pennetta, *Fluctuation and Noise Letters*, **2**, R29 (2002).

[20] C. Pennetta, E. Alfinito, L. Reggiani and S. Ruffo, *Physica A*, **340**, 380, (2004); C. Pennetta, E. Alfinito, L. Reggiani and S. Ruffo, *Semicond. Sci. Technol.*, **19**, S164 (2004).

[21] S. Zapperi, P. Ray, H. E. Stanley and A. Vespignani, *Phys. Rev. Lett.* **78**, 1408 (1997).

[22] G. Odor, *Rev. of Mod. Phys.* **76**, 663 (2004).

[23] T. Bodineau and B. Derrida, *Phys. Rev. Lett.*, **92**, 180601 (2004).

[24] C. Pennetta, G. Trefán and L. Reggiani, in *Unsolved Problems of Noise and Fluctuations*, ed. by D. Abbott, L. B. Kish, AIP Conf. Proc. **551**, New York (1999).

[25] C. Pennetta, E. Alfinito, L. Reggiani and S. Ruffo, in *Noise in Complex Systems and Stochastic Dynamics II*, p. 38, ed. by Z. Gingl and J. M. Sancho and L. Schimansky-Geier and J. Kertesz, Procs. SPIE, **5471**, Int. Soc. Opt. Eng., Bellingham (2004).

[26] C. Pennetta, E. Alfinito, L. Reggiani, F. Fantini, I. De Munari and A. Scorzoni, *Phys. Rev.* B, **70**, 174305 (2004).

[27] Z. Gingl, C. Pennetta, L. B. Kiss, and L. Reggiani, *Semic. Sci. Technol.*, **11**, 1770 (1996).

[28] C. Pennetta, L. Reggiani and G. Trefán, *Phys. Rev. Lett.*, **84**, 5006 (2000).

[29] R. Leturcq, D. L'Hôte, R. Tourbot, C. J. Mellor and M. Henini, *Phys. Rev. Lett.*, **90**, 076402 (2003).

[30] C. Grimaldi, T. Maeder, P. Ryser and S. Strässler, *J. Phys.D: Appl. Phys.*, **37**, 2170 (2004).

[31] K. Sieradzki, K. Bailey and T. L. Alford, *Appl. Phys. Lett.*, **79**, 3401 (2001).

[32] H. C. Kim, T. L. Alford and D. R. Alle, *Appl. Phys. Lett.*, **81**, 4287 (2002).

[33] M. M. Islam, E. Misra, H. C. Kim, M. Hasan and T. L. Alford, *IEEE Electron Device Lett.*, **25**, 19 (2004).

[34] Y. C. Zhang and S. Liang, *Phys. Rev.* B, **36**, 2345 (1987).

[35] P. Bak, C. Tang and K. Wiesenfeld, *Phys. Rev. Lett.*, **59**, 381 (1987); P. De Los Rios and Y. C. Zhang, *Phys. Rev. Lett.*, **82**, 472 (1999).

[36] J. Wang, S. Kadar, P. Jung and K. Showalter, *Phys. Rev. Lett.*, **82**, 855 (1999); S. S. Manna and D. V. Khakhar, *Phys. Rev.* E, **58**, R6935 (1998).

[37] B. Kaulakys and J. Ruseckas, *Phys. Rev.* E, **70**, 020101 (2004).
[38] L. B. Kiss and P. Svedlindh, *Phys. Rev. Lett.*, **71**, 2817 (1993).
[39] A. A. Snarskii, A. E. Morozovsky, A. Kolek and A. Kusy, *Phys. Rev.*E, **53**, 5596 (1996).
[40] M. Celasco and R. Eggenhöffner, *Eur. Phys. J.* B, **23**, 415 (2001).
[41] A. L. Rakhmanov, K.I. Kugel, Y.M. Blanter and M.Y. Kagan, *Phys. Rev.*B, **63**, 174424 (2001).
[42] B. I. Shklovskii, *Phys. Rev.* B, **67**, 045201 (2003).
[43] K. Shtengel and C. C. Yu, *Phys. Rev.* B, **67**, 165106 (2004).
[44] D. Sornette and C. Vanneste, *Phys. Rev. Lett.*, **68**, 612, (1992); C. Vanneste and D. Sornette, J. Phys. I (France), **2**, 16212, (1992).
[45] C. Pennetta, G. Trefan and L. Reggiani, *Phys. Rev. Lett.*, **85**, 5238 (2000).
[46] We take the correlation time associated with the fluctuations of the defect fraction, $\tau_p$ comparable with that corresponding to the fluctuations of the resistance, $\tau$, i.e. we take $\tau_p \approx \tau$. Our simulations confirm this assumption.
[47] A. Bunde, J. F. Eichner, S. Havlin and J. W. Kantelhardt, *Physica A*, **330**, 1 (2003).
[48] S. T. Bramwell, P. C. W. Holdsworth and J. F. Pinton, *Nature*, **396**, 552 (1998) and S. T. Bramwell, K.Christensen, J. Y. Fortin, P. C. W. Holdsworth, H. J. Jensen, S. Lise, J. M. López, M. Nicodemi, J. F. Pinton and M. Sellitto, *Phys. Rev. Lett.*, **84**, 3744 (2000).
[49] M. Clusel, J. Y. Fortin and P. C. W. Holdsworth, *Phys. Rev.* E, **70**, 046112 (2004).
[50] D. Sornette, *Critical Phenomena in Natural Sciences, Chaos, Fractals, Selforganization and Disorder: Concepts and Tools*, Springer, Berlin, (2004).
[51] C. Pennetta, *Eur. Phys. J.* B, **50**, 95 (2006).